Reachability Analysis of Dual Active Bridge DC-DC Converters

Heqiang Wang, Zefan Tang, Yan Li, Peng Zhang
Department of Electrical and Computer Engineering, University of Connecticut, Storrs, CT, USA 06269
Emails: heqiang.wang@uconn.edu, zefan.tang@uconn.edu, yan.7.li@uconn.edu, peng.zhang@uconn.edu

***Abstract*—This paper presents a reachability analysis approach for dual active bridge (DAB) converters in the presence of heterogeneous uncertainties induced by manufacturing tolerance, temperature, humidity, etc. The novelty of this paper includes: 1) it gives a comprehensive introduction of how to build a hybrid automata model for a DAB converter, and use the hybrid automata model for the purpose of reachability analysis through SpaceEx; 2) it develops the procedures of building the SpaceEx model for an arbitrary model by using Atom Text Editor; and 3) different non-deterministic input values are incorporated in the reachability analysis to further improve the performance. Test results validate the effectiveness and excellent performance of the presented method.**

***Index Terms*—Reachability analysis, dual active bridge, DC-DC converter, hybrid automaton, SpaceEx**

I. Introduction

The design and verification of new types of power electronic devices such as DC-DC converters require numerical simulations [1]. There are many types of simulation software tools that can offer the environment for users to model and test their designs, including Labview, Plexim PLECS, Simulink, and many more. However, only using simulations to analyze the models is intrinsically incomplete, because a simulation running one time only has a single execution of the system. Due to the infinite number of the initial conditions in the presence of heterogeneous uncertainties, just using simulations to test the designs of electronics devices can detrimentally increase the safety risk. For instance, Toyota Motor Corporation recalled nearly 1.9 million Prius cars in 2014 because of a mismatch between a boost converter and its software design. It is critical to develop a formal verification tool to consider all possible executions of the system with various uncertainties.

The formal verification community has developed many reachability analysis tools including UPPAAL, HyTech, PHAVer, SpaceEx, CORA, and HyLaa [2]–[7]. Among these tools, the SpaceEx is a widely used verification platform for hybrid automata. It combines polyhedra and supports function representations of continuous sets to compute an over-approximation of the reachable states [8]–[11]. For a reachability analysis using SpaceEx, a critical point is to build a SpaceEx model. A common method to build the SpaceEx model is using the HYbrid Source Transformer (HYST) to directly obtain this model [12]. However, for those complicated models such as the dual active bridge (DAB) converters, using HYST cannot accurately obtain the SpaceEx models [12], [13].

One modification of using SpaceEx for reachability analysis is to use the SpaceEx Model Editor to build the SpaceEx model by our own. The initial parameters and the related algorithms can be setup in the CFG file. But the SpaceEx Model Editor only has a few common available blocks with limited functions. Actually, to the best knowledge of the authors, no existing reachability analysis work has been done on complicated converters such as DAB converters.

This paper gives a comprehensive introduction of how to build a hybrid automata model for a DAB converter, and use the hybrid automata model for the purpose of reachability analysis through SpaceEx. It also develops the procedures of building the SpaceEx model for an arbitrary model including DAB converters by using Atom Text Editor. Moreover, the non-deterministic input values are incorporated in the reachability analysis to further improve the performance. Case studies are provided to validate the effectiveness and performance of the presented method.

The rest of this paper is organized as follows: Section II describes the DAB converters, and this is followed by the presented method for reachability analysis of DAB converters in Section III. Section IV provides the comparison results, and Section V concludes the paper.

II. System Description of DAB Converters

The circuit model of a typical DAB converter is given in Fig. 1. It consists of a primary bridge (PB), a secondary bridge (SB), and a transformer. Each bridge consists of four switches (S_1-S_4 or S_5-S_8). R_i represents the sum of switch on-resistances, line resistance, and transformer winding resistance. L is the transformer leakage inductance. C_0 and R_c are the shunt capacitor and its equivalent series resistance, respectively. V_{in} is the input DC voltage, and V_{out} is the output DC voltage on the final load R_0. V_p and V_s are the voltages at the two sides of the inductor L, and are used to control the switches. Using the parameters in Table I, Fig. 2 gives the waveforms of V_p and V_s under the single phase-shift (SPS) control, where the duty cycle D is set as 0.5, the period T is set as 20 μs, and the phase shift ϕ between V_p and V_s is $\pi/2$.

According to the status of the switches, the system operates in four modes, which are described as follows:

This work was supported in part by the National Science Foundation under Grant ECCS-1611095 and Grant ECCS-1831811, by the Department of Energy's Advanced Grid Modeling Program, by the Eversource Energy Center, and by funding from the Office of the Provost, University of Connecticut.

978-1-7281-0395-2/19/$31.00 ©2019 IEEE

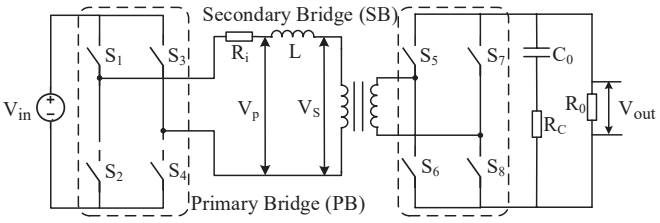

Fig. 1. The circuit model of a typical DAB converter.

TABLE I
PARAMETERS OF A DAB CONVERTER

Parameter	Value	Parameter	Value
V_{in}	30 V	R_0	12.5 Ω
L	35.49 μH	T	20 μs
R_i	0.38 Ω	D	0.5
R_c	0.45 Ω	C_0	455 μF

Mode 1: In this mode, the switches of the primary bridge S_1 and S_4, and the switches of the secondary bridge S_6 and S_7 are closed while the other switches are open during the switching cycle $[0, DT)$. The state variables are defined by the voltage across the capacitor v_C, and the current through the magnetizing inductor i_L. According to the Kirchoff's voltage law (KVL) and Kirchoff's current law (KCL), the ordinary differential equations (ODEs) of i_L and v_C are obtained as

$$\begin{cases} \frac{\mathrm{d}i_L}{\mathrm{d}t} = -\frac{R_t+R_0R_C/(R_0+R_C)}{L}i_L + \frac{R_0}{L(R_0+R_C)}v_C + \frac{1}{L}v_{in} \\ \frac{\mathrm{d}v_C}{\mathrm{d}t} = -\frac{R_0}{C_0(R_0+R_C)}i_L - \frac{1}{C_0R_0+R_C}v_C. \end{cases} \tag{1}$$

Mode 2: In this mode, the switches of the primary bridge S_1 and S_4, and the switches of the secondary bridge S_5 and S_8 are closed while the other switches are open during the switching cycle $[DT, T)$. Similarly,

$$\begin{cases} \frac{\mathrm{d}i_L}{\mathrm{d}t} = -\frac{R_t+R_0R_C/(R_0+R_C)}{L}i_L - \frac{R_0}{L(R_0+R_C)}v_C + \frac{1}{L}v_{in} \\ \frac{\mathrm{d}v_C}{\mathrm{d}t} = \frac{R_0}{C_0(R_0+R_C)}i_L - \frac{1}{C_0R_0+R_C}v_C. \end{cases} \tag{2}$$

Mode 3: In this mode, the switches of the primary bridge S_2 and S_3, and the switches of the secondary bridge S_5 and S_8 are closed while the other switches are open during the switching cycle $[T, (1+D)T)$. Similarly,

$$\begin{cases} \frac{\mathrm{d}i_L}{\mathrm{d}t} = -\frac{R_t+R_0R_C/(R_0+R_C)}{L}i_L - \frac{R_0}{L(R_0+R_C)}v_C - \frac{1}{L}v_{in} \\ \frac{\mathrm{d}v_C}{\mathrm{d}t} = \frac{R_0}{C_0(R_0+R_C)}i_L - \frac{1}{C_0R_0+R_C}v_C. \end{cases} \tag{3}$$

Mode 4: In this mode, the switches of the primary bridge S_2 and S_3, and the switches of the secondary bridge S_6 and S_7 are closed while the other switches are open during the switching cycle $[(1+D)T, 2T]$. Similarly,

$$\begin{cases} \frac{\mathrm{d}i_L}{\mathrm{d}t} = -\frac{R_t+R_0R_C/(R_0+R_C)}{L}i_L + \frac{R_0}{L(R_0+R_C)}v_C - \frac{1}{L}v_{in} \\ \frac{\mathrm{d}v_C}{\mathrm{d}t} = -\frac{R_0}{C_0(R_0+R_C)}i_L - \frac{1}{C_0R_0+R_C}v_C. \end{cases} \tag{4}$$

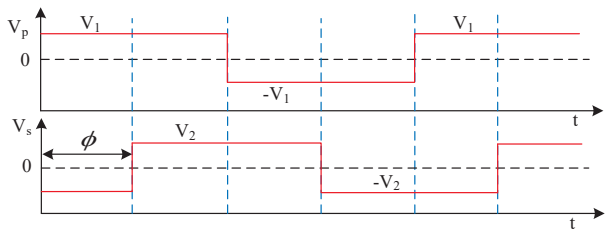

Fig. 2. The waveforms of V_p and V_s under the single phase-shift (SPS) control.

III. REACHABILITY ANALYSIS OF DAB CONVERTERS

In this section, the reachability analysis of a DAB DC-DC converter is presented, including 1) reachability algorithm, 2) SpaceEx description, 3) hybrid automation model of a DAB converter, and 4) DAB converter modeling in SpaceEx.

A. Reachability Algorithm

The reachability algorithm used in this paper is a classical fixed-point computation which is operated on symbolic states [5]. A symbolic state is a pair R = (l, Ω), where l is a location and Ω is a convex continuous set. The discrete post-operator $post_d(R)$ is defined as the set of states reachable by a discrete transition from R, and the continuous post-operator $post_c(R)$ is defined as the set of states reachable from R by letting an arbitrary amount of time elapse. The set of reachable states is the fixed-point of the sequence: $R_0 = post_c(Init)$ and $R_{k+1} := R_k \cup post_c(post_d(R_k))$. The algorithm uses a passed list of states found so far and a waiting list of states whose successors are yet to be computed. The flowchart of the algorithm is given in Fig. 3.

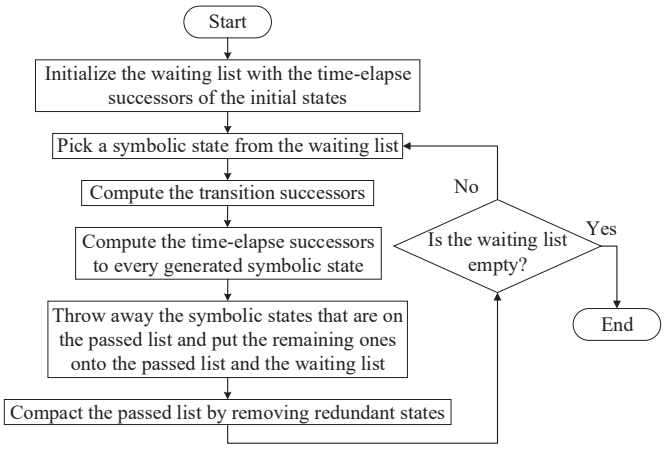

Fig. 3. Flowchart of the reachability algorithm.

B. SpaceEx Description

SpaceEx is a robust and user-friendly verification platform for hybrid systems. Its modeling language, called SX, is to allow the exchange of models with a graphical user interface and model editor, as well as the exchange with other tools and modeling languages via automatic translation. The SpaceEx consists of three components, namely, SpaceEx analysis core, web interface, and system model as shown in Fig. 4 [6].

- The analysis core is a program which takes a model file in SX and a configuration file in CFG. The configuration file specifies the initial states, the scenarios and other options and then analyzes the system and produces a series of output files.
- The web interface is a graphical user interface where users can use virtual machines to access the analysis core on the web server. It can be used to specify the initial states and other parameters, and can also visualize the output graphically.
- The model editor is a graphical editor for creating models of complex hybrid systems. While it can not well support the non-deterministic inputs.
- The Atom Text Editor is a text editor where users can directly edit and modify the SX file and the CFG file without using other hybrid system translation tools such as HYST [12].

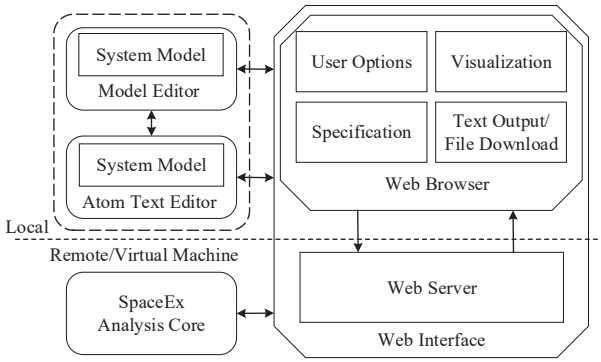

Fig. 4. Software architecture of the SpaceEx platform.

C. Hybrid Automaton Model of A DAB Converter

A hybrid automaton H can be defined by a tuple $\langle L, S, P, T, G, F, \rangle$, which are described as follows:

1) L is the infinite set of the topology that represents the control model of a hybrid system: $L = \{l_1, l_2, ..., l_n\}$. For a DAB converter in this paper, there are four modes which are therefore denoted as $L = \{l_1, l_2, l_3, l_4\}$.
2) S is a group of the continuous state variables: $S = \{i_L, V_C, t\}$, where t is the real time.
3) P is the set of the inputs to the system for each mode: $P = \{p_1, p_2, ..., p_n\}$. For a DAB converter in this paper, $P = \{[V_{in}, 0, 0]', [V_{in}, 0, 0]', [-V_{in}, 0, 0]', [-V_{in}, 0, 0]'\}$.
4) T is the set of feasible discrete transitions occurring among the modes. Each element is defined as $t_{ij} = (l_1, l_2) \in T$ which means there is a discrete transition from the i^{th} mode to the j^{th} mode. For a DAB converter in this paper, $T = \{(l_1, l_2), (l_2, l_3), (l_3, l_4), (l_4, l_1)\}$.
5) G is the guard set, which refers to the discrete transition from a given topology to another pre-defined topology. For a DAB converter in this paper, $G = \{(t \geq DT), (t \geq T), (t \geq (1+D)T), (t \geq 2T)\}$.
6) F is the set of ODEs that are defined for each topology $l \in L$ with the continuous state variable $s \in S$.

D. DAB Converter Modeling in SpaceEx

This paper develops an approach which uses the Atom Text Editor (see Fig. 4) to build the SpaceEx model for an arbitrary model including DAB converters. The flowchart of the presented method is given in Fig. 5. For an arbitrary model, its variables are defined step by step in the Atom Text Editor, and the SpaceEx model can thus be obtained. An example of the SpaceEx model for a DAB converter obtained via the presented method is illustrated in Fig. 6. The SX file of the SpaceEx model and the CFG file are then uploaded to the web server through the web interface as shown in Fig. 4. The reachability analysis is then implemented in the SpaceEx analysis core, and the results are sent back to the web interface.

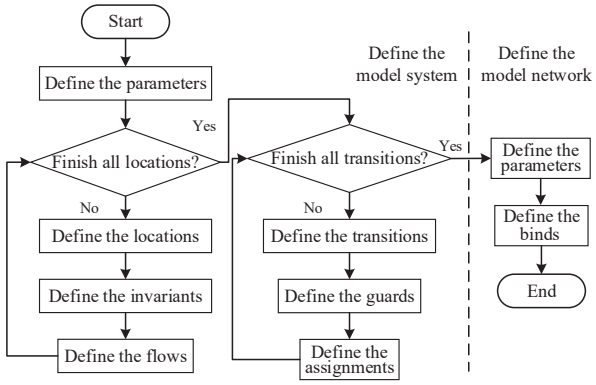

Fig. 5. Flowchart of the presented method.

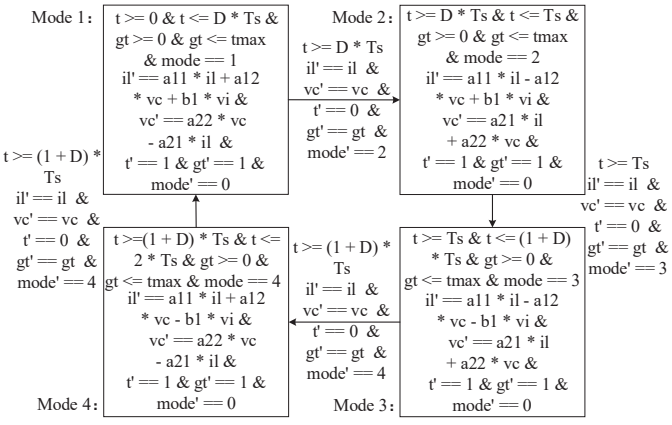

Fig. 6. The illustration of the SpaceEx model for DAB converters obtained via the presented method.

IV. Results and Analysis

This section presents the formal verification results of a DAB converter via verifying the states, e.g., i_L and v_C, which include: 1) comparison of Stateflow and SpaceEx; 2) reachability with different uncertainty levels of v_{in}; 3) reachability with non-deterministic v_C and i_L initial values; 4) reachability with deterministic and non-deterministic R_0; and 5) reachability with multiple and single non-deterministic inputs.

A. Comparison of Stateflow and SpaceEx

The traditional method to verify the performance of a DAB converter is to perform simulations using tools such as a combination of Stateflow and Simulink. Figs. 7-9 give the comparison results of Stateflow and SpaceEx, where v_{in} is determined as 30V in Stateflow and is within [29.95V, 30.05V] in SpaceEx. The other parameters of the DAB converter are the same as shown in Table I. It can be seen that the Stateflow results (see the blue dotted lines) are contained in the reachability set calculated by SpaceEx (see the black solid lines), which verifies that SpaceEx computes an over-approximation of the set of reachable states of the system, and in turn can be used to ensure that the system satisfies all desired safety properties for all possible executions.

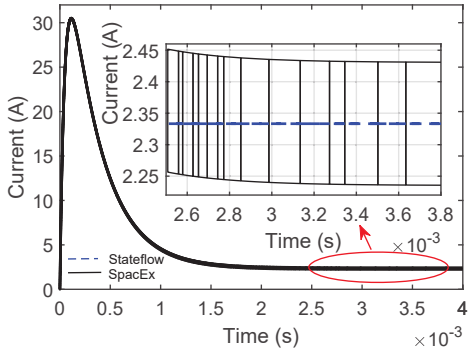

Fig. 7. Comparison results of Stateflow and SpaceEx on i_L.

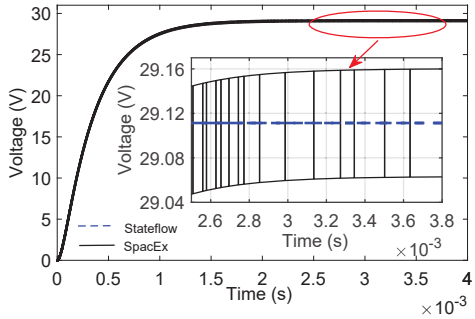

Fig. 8. Comparison results of Stateflow and SpaceEx on v_C.

B. Reachability with Different Uncertainty Levels of v_{in}

In reality, the different impacts of uncertainties (i.e., manufacturing tolerance, temperature, humidity, etc.) will result in different initial input values to the SpaceEx model. Considering the non-deterministic characteristics of the components' values, the non-deterministic initial input values are added for the reachability analysis. The non-deterministic value v_{in} is used in this subsection, where v_{in} is within [29.5V, 30.5V] for the high-level uncertainties and [29.95V, 30.05V] for the low-level uncertainties. The other parameters of the DAB converter are the same as shown in Table I. The reachability results with high-level input and low-level input are given in Figs. 10-12. It can be seen that compared with the low-level uncertainties input, the high-level uncertainties input gives a larger set of reachable states of the system, making the system satisfies desired safety properties for more possible executions.

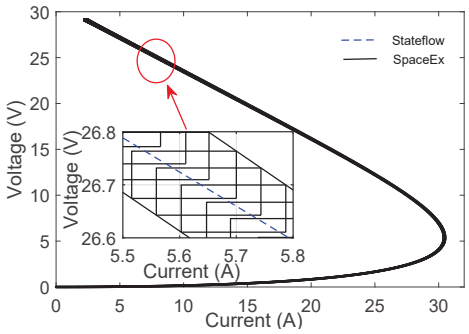

Fig. 9. Comparison results of Stateflow and SpaceEx on v_C and i_L.

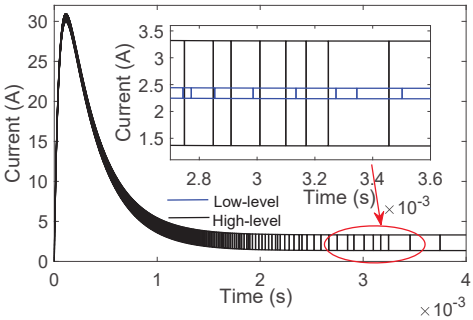

Fig. 10. Reachability results with high-level and low-level uncertainties input v_{in} on i_L.

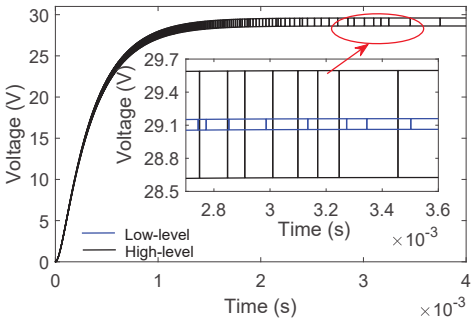

Fig. 11. Reachability results with high-level and low-level uncertainties input v_{in} on v_C.

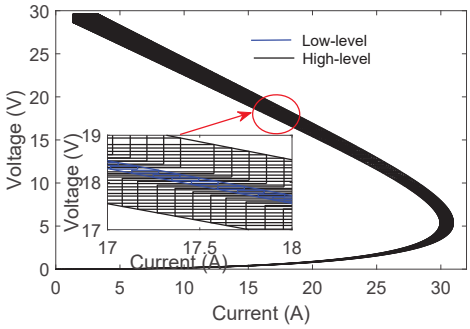

Fig. 12. Reachability results with high-level and low-level uncertainties input v_{in} on v_C and i_L.

C. Reachability with Non-deterministic v_C and i_L Initial Values

As shown in (1)-(4), there are three types of parameters that can affect v_C and i_L, namely, v_{in}, the initial values of v_C and i_L, and the weights such as R_o. Figs. 13-15 give the reachability results with different non-deterministic v_C and i_L initial values. In the one-side case, v_C is within [0V, 1.456V] and i_L is within [0A, 0.117A], while in the two-sides case, v_C is within [-1.456A, 1.456A] and i_L is within [-0.117A, 0.117A]. The other parameters of the DAB converter are the same as shown in Table I. It can be seen that the one-side results (see the blue dotted lines) are contained in the reachability set calculated by the two-sides results (see the black solid lines).

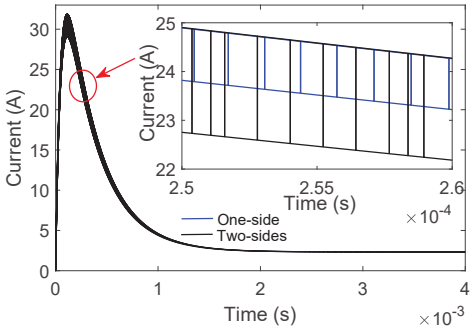

Fig. 13. Reachability results with non-deterministic v_C and i_L initial values on i_L.

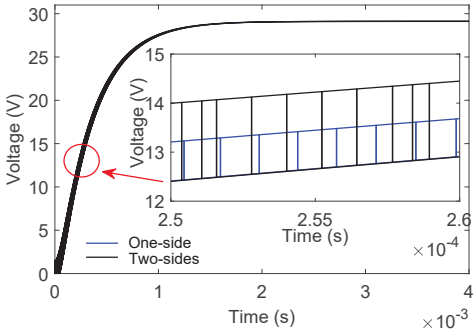

Fig. 14. Reachability results with non-deterministic v_C and i_L initial values on v_C.

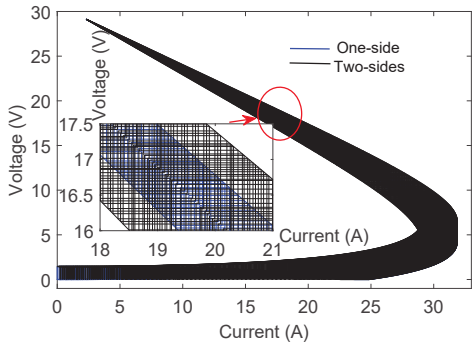

Fig. 15. Reachability results with non-deterministic v_C and i_L initial values on v_C and i_L.

D. Reachability with Deterministic and Non-deterministic R_0

Figs. 16-18 give the reachability results with deterministic and non-deterministic R_0, where the deterministic R_0 is set as 12.5Ω and the non-deterministic R_0 is within [11.25Ω,13.75Ω]. The other parameters of the DAB converter are the same as shown in Table I. It can be seen that compared with the deterministic R_0, the non-deterministic R_0 results in a larger set of reachable states of the system.

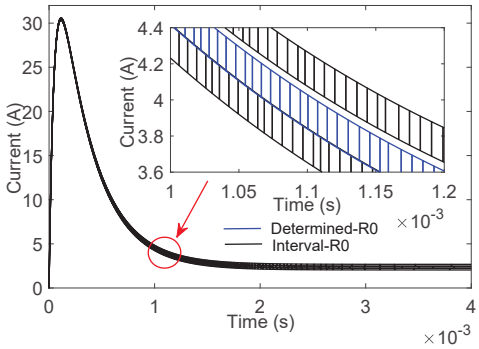

Fig. 16. Reachability results with deterministic and non-deterministic R_0 on i_L.

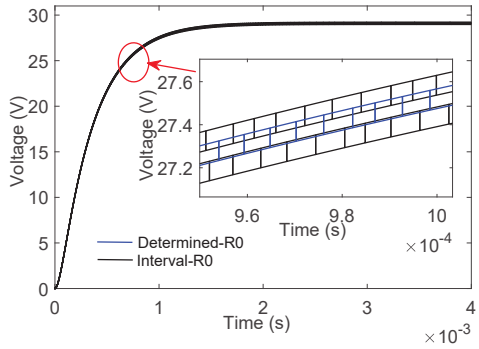

Fig. 17. Reachability results with deterministic and non-deterministic R_0 on v_C.

E. Reachability with Multiple Non-deterministic Inputs

To further evaluate the impacts of different parameters on reachability results, Figs. 19-21 give the comparison of reachability analysis using multiple non-deterministic inputs and a

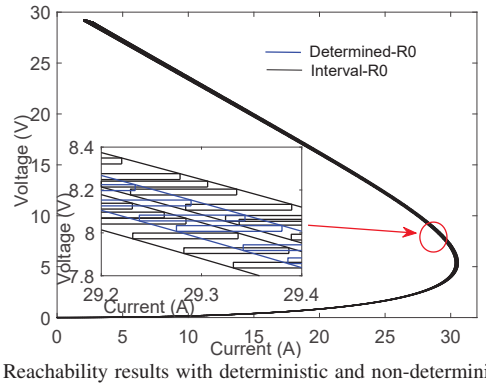

Fig. 18. Reachability results with deterministic and non-deterministic $R0$ on v_C and i_L.

single non-deterministic input. The red, green and blue curves represent the reachability results using the non-deterministic v_C and i_L, v_{in}, and R_0, respectively, and the black curves represent the reachability results using all the three types of parameters. It can be seen that 1) different parameters have different impacts; and 2) compared with using a single non-deterministic input, using multiple non-deterministic inputs gives a larger set of reachable states of the system.

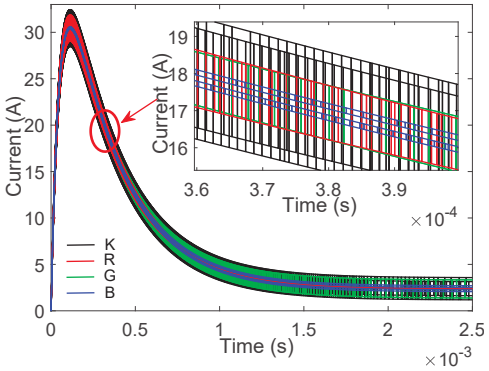

Fig. 19. Reachability results of multiple non-deterministic inputs and a single non-deterministic input on i_L.

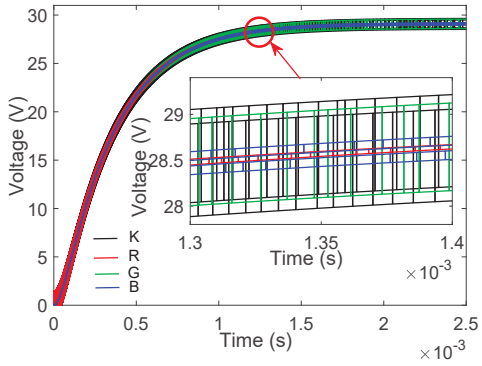

Fig. 20. Reachability results of multiple non-deterministic inputs and a single non-deterministic input on v_C.

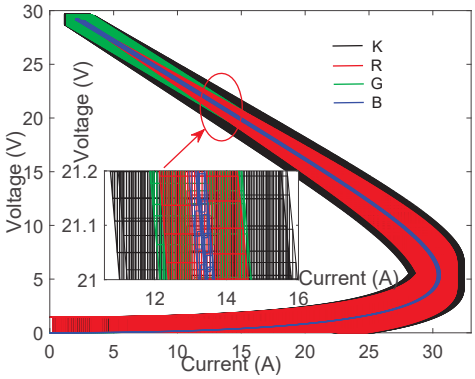

Fig. 21. Reachability results of multiple non-deterministic inputs and a single non-deterministic input on v_C and i_L.

V. Conclusion

This paper contributes a reachability analysis approach using SpaceEx for DAB converters. This work not only presents the procedures of reachability analysis for DAB converters, but also provides insightful situational awareness of power electronic devices in the presence of heterogeneous uncertainties. Future works include further evaluations of the presented method on more complicated designs, and more considerations on more realistic uncertainties.

References

[1] W. Han and L. Corradini, "Wide-range ZVS control technique for bidirectional dual-bridge series resonant dc-dc converters," *IEEE Transactions on Power Electronics*, 2019.

[2] G. Behrmann, A. David, and K. G. Larsen, "A tutorial on uppaal," in *Formal methods for the design of real-time systems*. Springer, 2004, pp. 200–236.

[3] T. A. Henzinger, P.-H. Ho, and H. Wong-Toi, "Hytech: A model checker for hybrid systems," *International Journal on Software Tools for Technology Transfer*, vol. 1, no. 1-2, pp. 110–122, 1997.

[4] G. Frehse, "Phaver: Algorithmic verification of hybrid systems past HyTech," in *International workshop on hybrid systems: computation and control*. Springer, 2005, pp. 258–273.

[5] G. Frehse, C. Le Guernic, A. Donzé, S. Cotton, R. Ray, O. Lebeltel, R. Ripado, A. Girard, T. Dang, and O. Maler, "SpaceEx: Scalable verification of hybrid systems," in *International Conference on Computer Aided Verification*. Springer, 2011, pp. 379–395.

[6] G. Frehse, "An introduction to SpaceEx v0. 8," *December*, 2010.

[7] S. Cotton, G. Frehse, and O. Lebeltel, "The SpaceEx modeling language," 2010.

[8] S. Bak and P. S. Duggirala, "Hylaa: A tool for computing simulation-equivalent reachability for linear systems," in *Proceedings of the 20th International Conference on Hybrid Systems: Computation and Control*. ACM, 2017, pp. 173–178.

[9] T. A. Henzinger, "The theory of hybrid automata," in *Verification of Digital and Hybrid Systems*. Springer, 2000, pp. 265–292.

[10] R. Alur, C. Courcoubetis, T. A. Henzinger, and P.-H. Ho, "Hybrid automata: An algorithmic approach to the specification and verification of hybrid systems," in *Hybrid systems*. Springer, 1993, pp. 209–229.

[11] T. A. Henzinger and V. Rusu, "Reachability verification for hybrid automata," in *International Workshop on Hybrid Systems: Computation and Control*. Springer, 1998, pp. 190–204.

[12] S. Bak, S. Bogomolov, and T. T. Johnson, "Hyst: A source transformation and translation tool for hybrid automaton models," in *Proceedings of the 18th International Conference on Hybrid Systems: Computation and Control*. ACM, 2015, pp. 128–133.

[13] S. Ling, L. Wanjun, L. Zhuoqiang, C. Yao, J. Huang, and W. Yue, "Stability analysis of digitally controlled dual active bridge converters," *Journal of Modern Power Systems and Clean Energy*, vol. 6, no. 2, pp. 375–383, 2018.